The Problems and Physics Prospects for a $\mu^+\mu^-$ Collider[1]

CAA-0137-3/97

David B. Cline

University of California, Los Angeles
Department of Physics and Astronomy, Box 951547
Los Angeles, CA 90095-1547 USA

Abstract. In 1992, a new study of $\mu^+\mu^-$ colliders was started at a workshop at Napa, California. Subsequently, many problelms have been solved except for two: (1) The best cooling system to use for the machine and (2) the real particle physics needs of such a machine. We argue here that these two issues are related and that the only compelling scientific argument today is for a $\mu^+\mu^-$ collider Higgs factory. We show that a 4-TeV collider may not even be the correct high-energy range based on the possible future observations at the LHC and the NLC and the Higgs factory. Such a collider requires very cold $\mu^{\pm}$ beams and will select the cooling method.

INTRODUCTION

A $\mu^+\mu^-$ collider offers some compelling particle physics opportunities at a tradeoff with immense technical problems (1,2). This is very similar to the situation for the $\bar{p}p$ collider where the scientific goals were clearly the *W*,*Z* discovery by Rubbia, McIntyre, and the author (3). The technical problem was to cool, store, reinject, accelerate, and collide the rare antiprotons, and this was a tour de force of accelerator physics carried out by the CERN and FNAL accelerator teams.

What are the similar scientific goals for a $\mu^+\mu^-$ collider? Some would say that we should blindly go to the highest energy (*i.e.*, 4 TeV). However, unlike 1976, there is no clear physics advantage of this energy, and the LHC will already have 14 TeV in the center of mass with a very high luminosity and years of detector operation before any 4-TeV $\mu^+\mu^-$ collider could be built. Current theory is very restrictive, suggesting that all new physics will occur below or at 1 TeV and, thus, this could be observed or totally rejected by 2010. In which case one may need 40 TeV or 400

[1]Presented at the symposium on Future High Energy Colliders, Part. '96 Sym 2 (Santa Barbara, CA, October 21-25, 1996) and to be published in the *Proceedings* by AIP.

In the next section, we discuss the Higgs collider, followed by our scheme to produce ultracold $\mu^{\pm}$ beams for the Higgs collider. Finally we give our conclusions.

A $\mu^+\mu^-$ COLLIDER HIGGS FACTORY

Recently there has been a great deal of activity concerning $\mu^+\mu^-$ colliders, starting with the Napa workshop in 1992 (4,5). We have proposed that such a collider is very useful to study the scalar sector of the electroweak interaction (2). In this brief report, we discuss the arguments for a Higgs factory (see Table 1).

The strongest argument for the low-energy 250 × 250-GeV collider comes from the growing evidence that the Higgs should exist in this low-mass range from:

1. The original works of Cabibbo and colleagues (6), which shows that, when $m_t > M_Z$ and assuming a grand unification theory (GUT), $M_H < 2\,M_Z$ (6);
2. Fits to LEP data imply that a low mass h^0 could be consistent with $m_t > 150$ GeV (7);
3. The extrapolation to the GUT scale that is consistent with SUSY also implies that one of the Higgs should have a low mass, perhaps below 130-150 GeV (7).

This evidence implies the exciting possibility that the Higgs mass is just beyond the reach of LEP II and in a range that is very difficult for the LHC to detect (1).

We expect the supercollider LHC to extract the signal from background (*i.e.*, seeing either $h^0 \to \gamma\gamma$ or the very rare $h^0 \to \mu\mu\mu\mu$ in this mass range, since $h \to b\bar{b}$ is swamped by hadronic background). However, detectors for the LHC are designed to extract this signal. Figure 1 gives a picture of the various physics thresholds that may be of interest for a $\mu^+\mu^-$ collider. In this low mass region, the Higgs is also expected to be a fairly narrow resonance and, thus, the signal should stand out clearly from the background from

$$\mu^+\mu^- \to \gamma \to b\bar{b} \to Z_{\text{tail}} \to b\bar{b} \quad . \tag{1}$$

For masses above 180 GeV, the dominant Higgs decay is

$$h^0 \to W^+W^- \quad \text{or} \quad Z^0Z^0 \quad , \tag{2}$$

and the LHC should easily detect this Higgs particle. Thus the $\mu\mu$ collider is better adapted for the low mass region. The report of Barger *et al.* is very illuminating regarding the physics potential of a $\mu\mu$ collider (see Table 2) (1,7,8).

TABLE 1. Arguments for a $\mu^+\mu^-$ Collider Higgs Factory

1. The m_μ/m_e ratio gives coupling 40,000 times greater to the Higgs particle. In the SUSY model, one Higgs m_h < 120 GeV!!
2. The low radiation of the beams makes precision energy scans possible.
3. The cost of a "custom" collider ring is a small fraction of the $\mu^\pm$ source.
4. Feasibility report to Snowmass established that $\mathcal{L} \sim 10^{33}$ cm^{-2} s^{-1} is feasible.

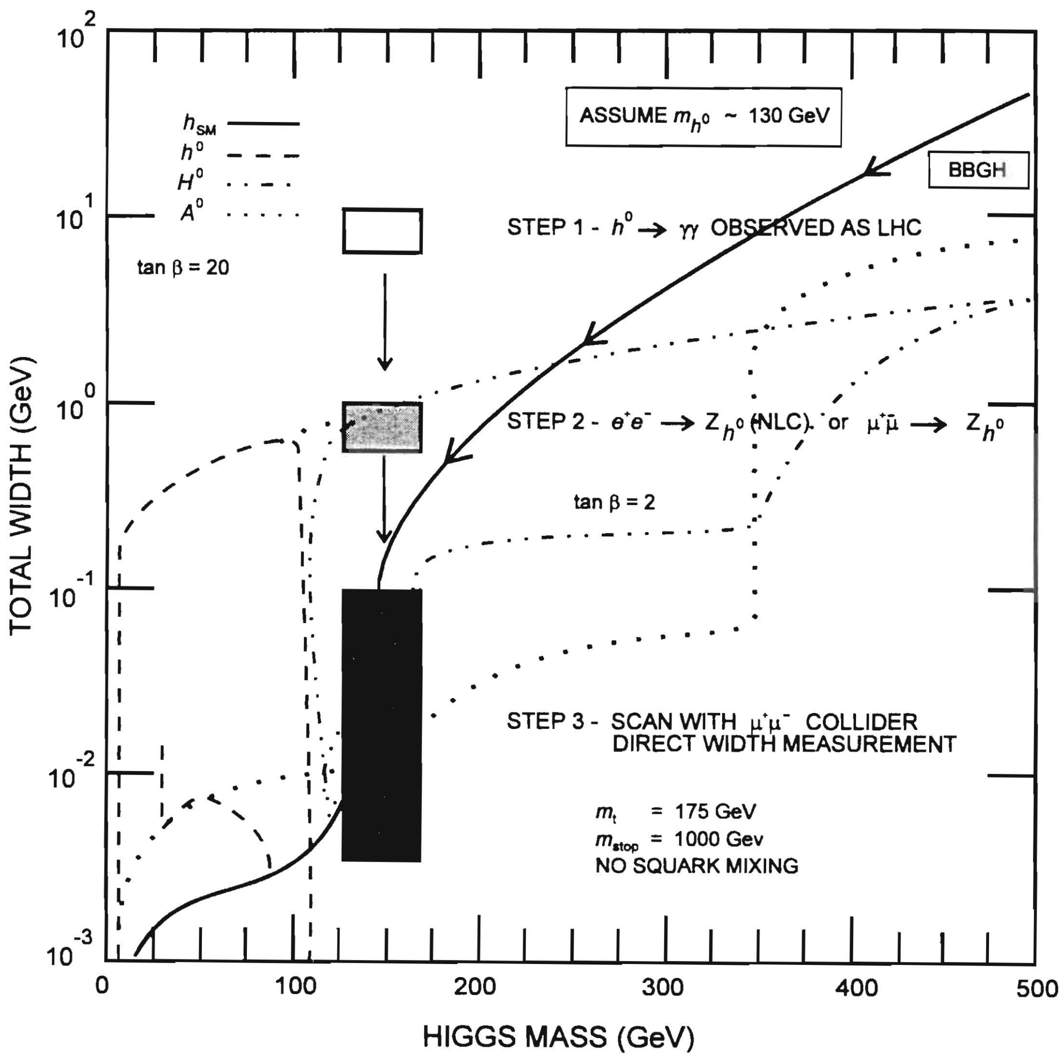

FIGURE 1. A $\mu^+\mu^-$ collider Higgs-factory concept. The Higgs is discovered at the LHC (CMS) and the width further reduced at the NLC or at a $\mu^+\mu^-$ collider. The final stage is to scan for the Higgs at the $\mu^+\mu^-$ collider. Existing models can be distinguished by their widths. [Adapted from (7) (BBGH = Barger, Berger, Gunion, Han) and (9).]

TABLE 2. The Scalar Sector

With a high-mass *t* quark, precision LEP/SLD data and the theorists' dreams of a SUSY world, the scalar (pseudo-scalar sector) is possibly very complex and may require several types of colliders.[8] Consider:

- If the low-mass Higgs has $m > 130$ GeV, MSSM is not allowed.
- If $m > 200$ GeV, there are constraints from the requirement that perturbation theory be useful up to very high energy and from the stability of the vacuum.
- If $m < 130$ GeV, MSSM is possibly ok, but we may expect other particles (*H*, *A*), and the width of the low mass Higgs may change.
- The scalar sector may be extremely complex, requiring *pp* (LHC) and $\mu^+\mu^-$ colliders (and possibly NLC and $\gamma\gamma$ colliders).
- In high energy collisions, vector states are allowed unless a special method is used. Consider $\mu^+\mu^-$ colliders with polarized $\mu^{\pm}$:

$\mu^+\mu^-$ <
- (100-500) GeV - scalars (*H*, *A*, ...) W^+W^-
- $\geq 2 +$ TeV Z^0Z^0 production in scalars

This cannot be done for *pp* or e^+e^- colliders.

- A $\mu^+\mu^-$ collider is complimentary to the LHC/CMS detector.

Scan for Higgs Mass and Width: SUSY or Not

In this section, we assume for the sake of argument that the CMS detector at the LHC has barely detected a signal at $m \sim 130$ GeV ($h^0 \to \gamma\gamma$) and at an experimental width of ~8 GeV (Step 1, illustrated in Fig. 1). The question will now be

1. Is this a Higgs boson or not?
2. Is it the standard model Higgs or a SUSY Higgs?

We envision the next step would be to construct the $\mu^+\mu^-$ collider operating between the energies of $E_{\mu^+\mu^-} \sim m_{h^0}$ (CMS) and $E_{\mu^+\mu^-} \sim m_Z + m_{h^0}$ (CMS) or the use of the NLC to observe $e^+e^- \to Z^0h^0$ (10). We build the $\mu^+\mu^-$ collider (after already having built a $\mu^{\pm}$ source), and for Step 2 operate near the $Z^0 + h^0$ (CMS) threshold to determine m_{h^0} and Γ_{h^0} to ~ 1 GeV. (See Fig. 2 for the cross sections.) For Step 3, we envision an energy scan of the mass region by varying the $\mu^+\mu^-$ energy (1,9). At some point, the mass and width are determined and then used to distinguish between the standard model Higgs and a SUSY Higgs (Fig. 3).

The final step is to measure the branching fractions for different decay modes (6,7). Figure 4 shows the expectations for the standard model Higgs.

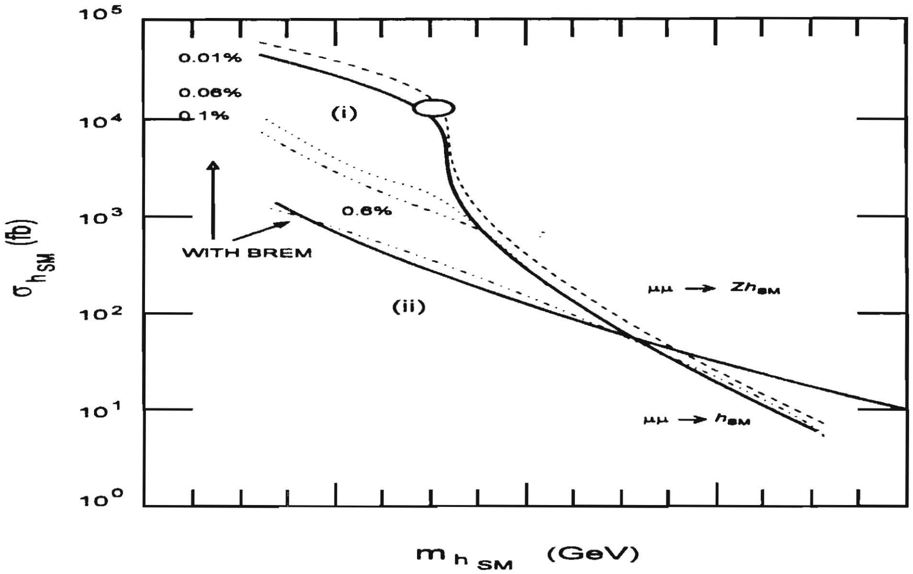

FIGURE 2. Cross sections versus $m_{h_{SM}}$ for inclusive standard-model Higgs production: (i) the s-channel $\bar{\sigma}_h$ for $\mu^+\mu^- \to h_{SM}$ with $R = 0.01\%$, 0.06%, 0.1%, and 0.6%; and (ii) $\sigma(\mu^+\mu^- \to Z_{h_{SM}})$ at $\sqrt{s} = m_Z + \sqrt{2}\, m_{h_{SM}}$. Also shown is the result for $R = 0.01\%$ if bremsstrahlung effects are not included. [Adapted from (7).]

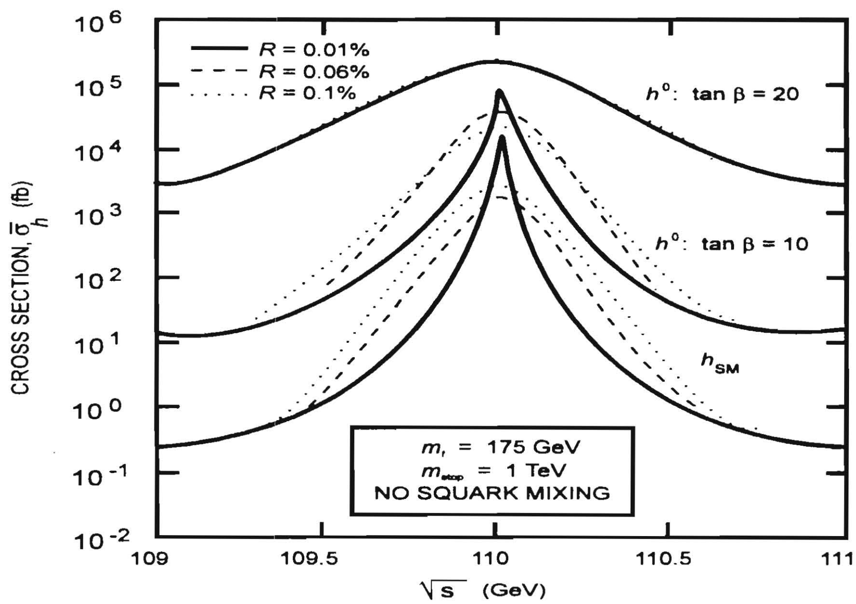

FIGURE 3. The effective cross section, $\bar{\sigma}_h$, obtained after convoluting σ_h with the Gaussian distributions for $R = 0.01\%$, 0.06%, and 0.1%, is plotted as a function of $\sqrt{s}$ taking $m_h = 110$ GeV. Results are displayed in the cases h_{SM}, h^0 with tan $\beta = 10$ and = 20. In the MSSM h^0 cases, two-loop/RGE-improved radiative corrections have been included for Higgs masses, mixing angles, and self-couplings assuming = 1 TeV and neglecting squark mixing. The effects of bremsstrahlung are not included in this figure. [Adapted from (7).]

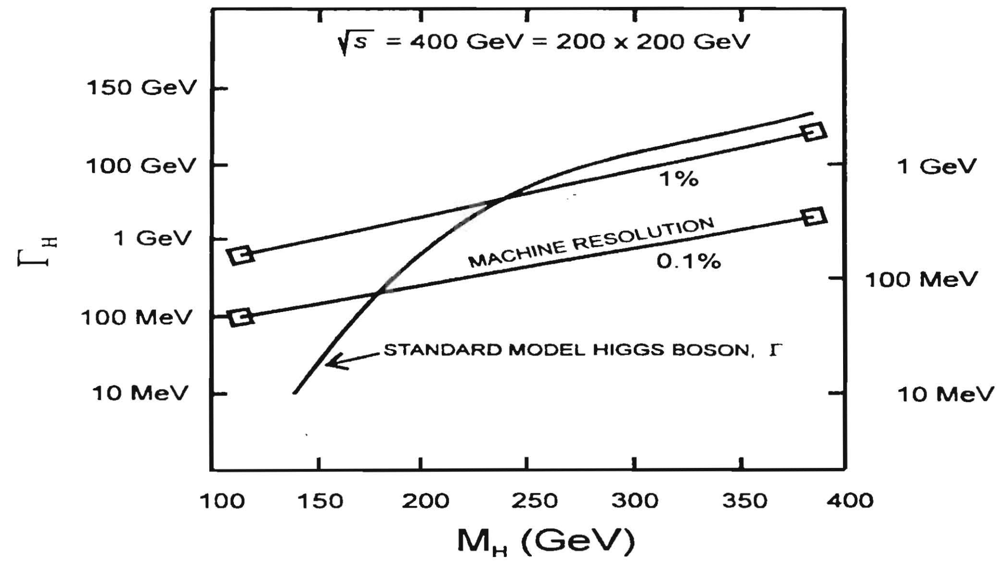

FIGURE 4. Machine requirements for Higgs scan (11).

Polarized Collider

The most interesting question now in particle physics is associated with the origin of mass. It is generally assumed that the exchange of fundamental scalar particles, called the "scalar sector'" is somehow responsible for this. For super-symmetry modes, this scalar sector is even more complex and interesting (see Table 2) (11,12).

In this section, we highlight one of the most interesting goals of a $\mu^+\mu^-$ collider: the discovery of a Higgs boson in the mass range beyond that to be covered by LEP I & II (~ 80 - 90 GeV) and the natural range of the supercolliders.

There are several ways to determine the approximate mass of the Higgs boson in the future (10). Suppose it is expected to be at a mass of 135 ± 2 GeV, the energy spread of a $\mu^+\mu^-$ collider can be matched to the expected width (see Fig. 5). An energy scan could yield a strong signal to background especially with polarized $\mu^+\mu^-$ in the scalar configuration [11,12]. Once the Higgs is found, the following could be carried out:

1. Measurement of width, to separate standard-model Higgs from SUSY or other Higgs models (6,7),

2. Measurement of the Branching fractions, the rare decay will involve loop effects that can sample very high energies.

Polarization will play an essential role for any $\mu^+\mu^-$ collider (12,13)!

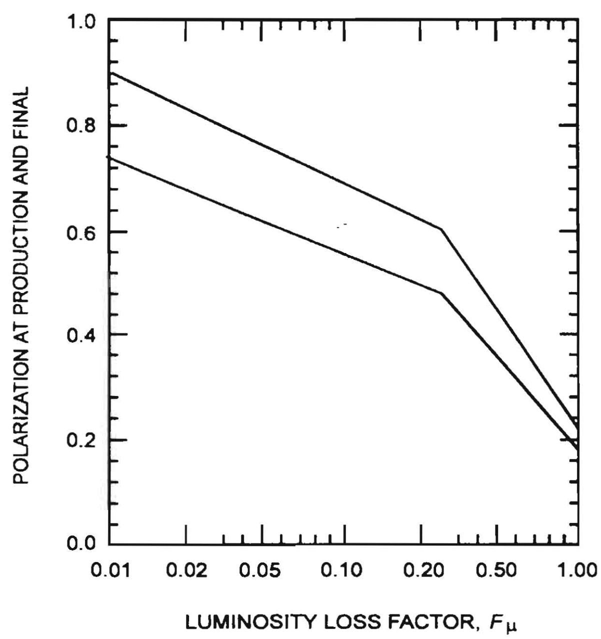

FIGURE 5. Polarization vs the fraction, F_μ, of muons accepted (solid line: polarization at source; dashed line: after cooling) (8).

Polarization is natural for $\mu^\pm$ since they are produced in weak decays and are initially fully polarized because of this V-A interaction. There are three proposed methods for producing intense polarized $\mu^\pm$ beams:

- Accelerate polarization and cool the $\pi^\pm$ (A. Skrinsky *et al.*) (14),
- Use $K^\pm$ decays and "narrow-band neutrino-like beam," and
- Use pion decays and a short proton bunch (9).

Figure 5 shows the tradeoff between intensity and polarization in one of these schemes (9,12,14). This is one of the major areas of research for $\mu^+\mu^-$ colliders.

Some Examples of Possible $\mu^+\mu^-$ Colliders for Higgs Factories

At the Snowmass '96 meeting, the U.S. $\mu^+\mu^-$ collider consortium presented a feasibility design of a $\mu^+\mu^-$ collider (9). The important point is that $\mathcal{L} \sim 10^{33}$ cm^{-2} s^{-1} was shown to be possible for this collider. We consider this an existence of proof of sorts. This collider is complex, the simplest part being the actual storage ring for the $\mu^+\mu^-$ collisions. It is important to note that this collider ring is likely a minor part of the cost of the overall complex.

There are other possible $\mu^+\mu^-$ collider designs that may serve as a Higgs factory. These designs differ by either the assumptions about the $\mu^\pm$ cooling method or the type of overall collider. Figure 6(A) shows a schematic design for a $\mu^+\mu^-$ collider in Japan that uses the high-current 50-GeV accelerator now being designed for KEK (15). The cooling method is by frictional cooling of low-energy $\mu^\pm$ beams.

Figure 6(B) shows a scheme worked out by the author and A. Bogacz, which uses crystal channeling for both the cooling and the collisions (16). In the latter case, if the $\mu^\pm$ can be confined to a crystal channel (~ 10 – 30 Å) then high luminosity can be achieved using modest $\mu^\pm$ intensities, greatly reducing the background and possible cost of the Higgs factory.

A hypothetical schedule for a Higgs-factory $\mu^+\mu^-$ collider is given in Table 3, which is of course entirely the author's own viewpoint.

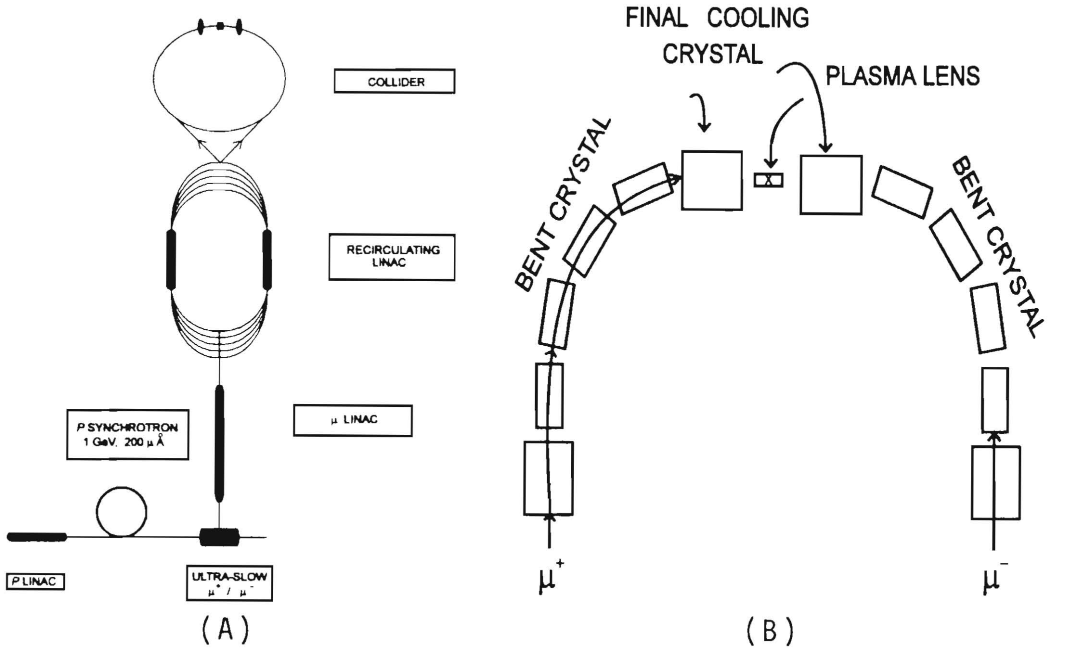

FIGURE 6. Collider concepts: (A) Japanese $\mu^+\mu^-$ collider (15); (B) Crystal quantum collider (16).

TABLE 3. Possible Scheme for a $\mu^+\mu^-$ Collider Higgs Factory

~ 2003:	Start construction of $\mu^\pm$ source.
~ 2006:	First observation of h^0 in CMS (ATLAS).
~ 2007:	Design final collider; start construction.
~ 2009:	Higgs factory operates; scan for h^0.
~ 2010:	→ 10^5 h^0 in direct channel.

FINAL CRYSTAL COOLING TO REDUCE THE BEAM CURRENT AND DETECTOR BACKGROUNDS FOR A $\mu^+\mu^-$ COLLIDER

Over the past four years the possibility of a real $\mu^+\mu^-$ collider has gained interest (1,17,18). With the *Proceedings* of the 1995 San Francisco conference (8) and the "Snowmass Book" (9), the design goals have gained even more credibility. However, there are several serious problems still remaining:

1. The high backgrounds in the detector from $\mu^{\pm}$ decay products (1,17,18),
2. The very high $\mu^{\pm}$ content in the final collider ($\sim 5 \times 10^{12}$ $\mu^{\pm}$ per bunch),
3. The relatively poor reduction of the phase-space using medium energy ionization cooling (18), and
4. The current high cost of the source due to the large yield of $\mu^{\pm}$ required to reach high luminosity.

Most of these problems can be partially cured if the number of $\mu^{\pm}$ required to produce high luminosity can be reduced.

Over the past few years we have studied the use of crystal channels for cooling (19,20) and even for a $\mu^+\mu^-$ collider that would use bent-crystal beam confinement. Here, we show how crystal cooling for the high-energy $\mu^{\pm}$ beams could result in a dramatic decrease in the beam emittance and, therefore, provide high luminosity with a substantially reduced beam intensity and backgrounds of $\mu^{\pm}$ in the storage ring (1,17). Also, reducing the beam emittance at high energy helps the relatively poor low-energy beam cooling (12). Finally, the lower yield of $\mu^{\pm}$ reduces the required proton current in the $\mu^{\pm}$ source, thus possibly reducing considerably the cost of the overall $\mu^+\mu^-$ collider (8).

We now turn to a discussion of the cooling concept. Our model calculation, presented here, shows that one can decrease the normalized emittance to less than $\epsilon_N = 10^{-8}$ mrad by passing the muon beam through a cascade of many cooling modules.

Crystal-Channel Beam Cooling

We consider motion of planar channeled particles in a crystal, which is bent elasticity in a direction perpendicular to the particle velocity and to the channeling planes. The effect of bending introduces a centripetal force to the equation of transverse motion (21) (by adding a linear piece to the crystal potential), which is equivalent to lowering one side of the continuum potential well and raising the other. The equilibrium planar trajectory moves away from the midpoint of the planar channel toward the plane on the convex side of the curved planar channel. However, such a shift would cause some fraction of the channeled particles to leave the potential well (dechannel) (22). The curvature at which no particle can remain channeled is reached when the equilibrium point of planar channeled motion is shifted to the position of the planar wall on the outside of the curve. This critical radius of curvature, known as the Tsyganov radius (23), ρ_T, is

$$\rho_T = \frac{2E_\mu}{\phi a} \quad , \tag{3}$$

where $\phi = 6 \times 10^{12}$ GeV m^{-2} is a material constant, related to the curvature of the potential well (24), and a is the distance between adjacent atomic planes (≈2 Å).

Using a simple formula linking equivalent magnetic bending field, B, with the trajectory's curvature, ρ, namely

$$B[\text{tesla}] \times \rho_T[\text{m}] = 3.34 \times E_\mu[\text{GeV}] \quad , \tag{4}$$

one can calculate the maximum available equivalent bending field corresponding to the Tsyganov curvature. From Eqs. (3) and (4), this field is given by

$$B_T[\text{tesla}] = 3.34 \times (1/2)\phi a \quad . \tag{5}$$

Its numerical value for silicon is evaluated as $B_T = 2 \times 10^3$ tesla. We note in passing, that the maximum bending field is energy independent.

Here we propose a fast muon-cooling scheme based on the ionization energy loss (25) experienced by high-energy muons (25 GeV) channeling through an Si crystal. Applying classical theory of ionization energy loss (4(A)), a relativistic (γ) charged particle passing through an Si crystal of length, ΔL, loses total energy of ΔE[MeV] $= 4 \times 10^2 \times \Delta L$[m]. One can introduce a characteristic damping length, Λ,

$$\frac{1}{\Lambda} = \frac{1}{E_\mu}\frac{\Delta E}{\Delta L} \quad , \tag{6}$$

over which the particle loses all its energy. Relativistic muons passing though the crystal lose energy uniformly in both the transverse and longitudinal directions according to Eq. (6). After passing through a short section of a crystal ($\Delta L \ll \Lambda$), muons are re-accelerated longitudinally to compensate for the lost longitudinal energy. This leads to the transverse emittance shrinkage.

Introducing normalized transverse emittance, $\epsilon_N = \gamma\, \sigma_x\, \sigma_{x'}$, one can write the normalized emittance budget in the form of the following cooling/heating equation:

$$\frac{d\epsilon_N}{dL} = -\frac{\epsilon_N}{\Lambda} + \left(\frac{\Delta\epsilon_N}{\Delta L}\right)_{\text{scatt}} \quad . \tag{7}$$

The last term in the above equation accounts for transverse heating processes contributing to the beam divergence increase according to the following relationship (24):

$$\left(\frac{\Delta\epsilon_N}{\Delta L}\right)_{\text{scatt}} = \frac{1}{2}\gamma\beta\,\frac{\Delta\langle\theta\rangle^2_{\text{scatt}}}{\Delta L} \quad . \tag{8}$$

Here β is the beta function of a focusing crystal channel, which has an enormously small value ($\beta = 2 \times 10^{-6}$ m, for 25-GeV muons channeling through a silicon crystal).

For muon channeling in a dielectric crystal, the dominant scattering process comes from elastic (Rutherford) muon scattering off the conduction electrons present in the channel. One can integrate the Rutherford cross section over the solid angle, which yields the following formula:

$$\alpha = \left(\frac{\Delta\epsilon_N}{\Delta L}\right)_{\text{scatt}} = 40\pi n\,\frac{r_\mu^2}{\gamma}\,\beta \quad . \tag{9}$$

Here $r_\mu = 1.4 \times 10^{-17}$ m is the classical muon radius and $n = 6 \times 10^{29}$ m^{-3} is the average concentration of the conduction electron gas in silicon crystal.

Integrating the cooling equation, Eq. (7), one obtains the following compact solution in terms of the normalized transverse emittance evolution:

$$\epsilon_N = \epsilon_N^0\, e^{-(L/\Lambda)} + \Lambda\alpha\left[1 - e^{-(L/\Lambda)}\right] \quad . \tag{10}$$

The last term in Eq. (10) sets the equilibrium cooling limit of

$$\epsilon_N^{\text{min}} = \Lambda\alpha \quad , \quad L \rightarrow \infty \quad . \tag{11}$$

Assuming 25-GeV muons, one gets $\Lambda = 62.5$ m and the equilibrium limit of the normalized emittance of

$$\epsilon_N^{\text{min}} = 8 \times 10^{-9} \text{ mrad} \quad . \tag{12}$$

This value of the normalized emittance will be used in our achievable luminosity estimate.

Bent-Crystal Cooling Ring

Here we employ previously discussed properties of the planar channeling of high energy muons in silicon to design components of a storage ring. Particularly, we are interested in a section of bent crystal followed by two straight pieces providing alternating horizontal-vertical focusing. A basic guiding cell is depicted schematically in Fig. 7. It can be noticed that the induced configuration of guiding fields in this element is equivalent to a powerful alternating gradient achromat.

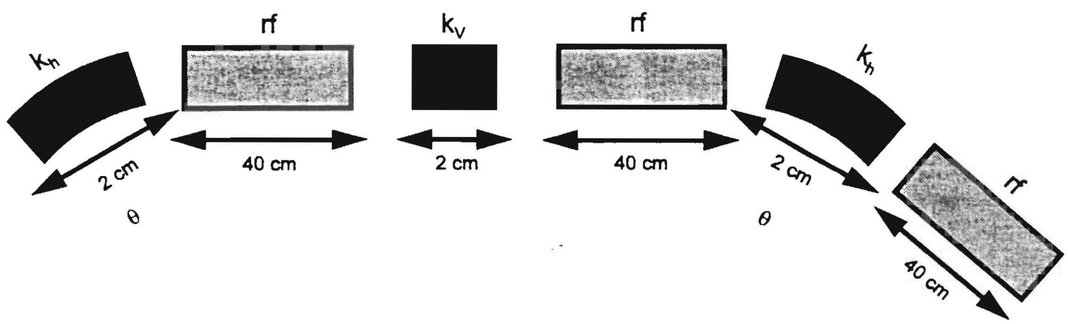

FIGURE 7. Layout of a cooling ring consisting of 50 bending-focusing-acceleration multi-functional cells. A straight piece of Si crystal rotated by 90° separating two sections of bent crystals provides vertical focusing, which maintains betatron phase stability in the proposed lattice. Conventional rf, 40-cm-long inserts (20 MeV/m) follow every 2-cm-long section of Si crystal absorber. (E_μ = 25 GeV, $k_h = k_v = 180\ m^{-2}$, $\theta = 2\pi \times 10^{-2}$ rad, rf grad = 20 MeV/m)

Relativistic muons channeling through an Si crystal are confined between two neighboring atomic planes - they experience strong focusing electrostatic crystal potential in the direction perpendicular to these planes, while there is virtually no confinement in the direction parallel to the planes (no focusing or defocusing). The focusing gradient, $k = 1/\beta$, is equivalent to the magnetic quadrupole strength, k_1 (magnetic gradient), where

$$k_1 = \frac{1}{B\rho}\frac{\partial By}{\partial x} \quad , \tag{13}$$

and

$$k = \frac{\phi}{E_\mu} \quad . \tag{14}$$

E_μ is the total muon energy and $\phi = 6 \times 10^{12}$ GeV m^{-2} is a material constant, related to the curvature of the potential well. Assuming 25-GeV muons, crystal focusing gradient, k, yields an enormous value of 180 m^{-2}, exceeding conventional quadrupole strength by four or five orders of magnitude.

As discussed previously in "Crystal Channel Beam Cooling," the crystal can be bent slightly, so that channeling muons follow the curvature of the guiding field, which results in bending of muon trajectories similar to the effect of a bending magnetic field. Projecting experimental results for proton channeling in a bent silicon crystal, one can assume that 25-GeV muons channeling through a 2-cm-long crystal should follow (without significant dechanneling effects) a bend of $\theta = 2\pi \times 10^{-2}$ rad (compared with the critical bending angle $\theta_T = 2 \times 10^{-1}$ rad). The lattice design presented here is based on these two numbers, k and θ.

Figure 7 illustrates a functional bending-focusing cell, where alternating sections of the horizontal and vertical continuous focusing channels are combined with sections of horizontally bent Si crystals. The following is the sequence of crystal elements: a horizontally focusing bent crystal (2-cm long) - a short drift space - a conventional rf re-acceleration section (40-cm long) - a short (2-cm long) vertically focusing straight crystal - a short drift space - another conventional rf re-acceleration section (40-cm long) - and finally, a horizontally focusing bent crystal (2-cm long) followed by a conventional rf re-acceleration section (40-cm long) completes the proposed elementary cell. At 25 GeV, one could close the entire collider ring using 50 of the above $F_hOF_vOF_hO$ cells. For a sequence of the above described cells, one can find periodic betatron trajectories in both the horizontal and vertical planes - the betatron phase stability is provided by the proposed lattice configuration (alternating horizontal/vertical focusing). By virtue of [110] planar channeling, discussed in detail in the previous section, a crystal channel provides an ultra-strong electrostatic focusing gradient in the [110] direction with practically no confinement or defocusing in the plane perpendicular to the [110] direction. This fact guarantees both local and global decoupling of the horizontal and vertical betatron motions for the proposed collider lattice.

Practical realization of muon cooling at 25 GeV could be done in a compact "cooling ring." Assuming characteristic damping length, Λ, of 62.5 m, the energy loss suffered by the muon beam after passing through a 2-cm-long section of an Si crystal is equal to 8 MeV. In principle, conventional high-gradient (20-MeV/m) acceleration inserts (a 40-cm-long rf insert following every 2-cm-long crystal absorber) could be used to replenish the suffered energy loss (0.4 m $\times$ 20 MeV/m = 8 MeV). The proposed cooling ring of 50-fold symmetry would have a nominal circumference of 63 meters!

Our goal is to start with the initial muon phase-space of the normalized emittance of 2.5×10^{-7} mrad and cool it down to the final emittance of 2.5×10^{-9} mrad. One can see from Eq. (10) that to achieve this goal, muons have to pass through the total silicon crystal length of

$$L = 2 \log 10 \times \Lambda = 280 \text{ m} \quad . \qquad (15)$$

In the proposed cooling cell architecture, the total cooling medium (silicon) length of L = 280 m is equivalent to about 90 turns of the beam circulation in the ring. The lost energy is replenished every ΔL = 2 cm, which satisfies the adiabatic re-acceleration condition ($\Delta L \ll \Lambda$ = 62.5 m).

To go beyond the above simple analytic calculation, we are planning to carry out realistic computer simulations of planar channeling in bent crystals. One should track a charged particle through the distorted crystal lattice with the use of a realistic continuous-potential approximation and take into account the processes of both single and multiple scattering of electrons and nuclei, as well as on various defects and imperfections of the crystal lattice.

Application To High Energy Cooling: Conclusions

In this section, we show how crystal cooling for the high energy $\mu^{\pm}$ beams could result in a dramatic decrease in the beam emittance and, therefore, would provide high luminosity with a substantially reduced beam intensity and backgrounds of $\mu^{\pm}$ in the storage ring. Also, reducing the beam emittance at high energy helps the relatively poor low-energy beam cooling. Finally, the lower yield of $\mu^{\pm}$ reduces the required proton current in the $\mu^{\pm}$ source, thus possibly considerably reducing the cost of the overall $\mu^{+}\mu^{-}$ collider.

We suggest employing ionization energy loss in an alternating focusing crystal channel as a cooling mechanism, since initially small muon phase-space allows for efficient channeling through long sections of silicon crystal. Ultra-strong focusing in a crystal channel combined with alternating bending makes it a powerful focusing cell with ultra-small beta function. The cooling equation derived here shows that it is quite feasible to reduce transverse emittance by two orders of magnitude. Our model calculation done for 25 GeV muons shows that final emittances as low as 10^{-9} mrad are readily achievable, limited only by multiple scattering off the valence electrons in the crystal.

We conclude our study with the following observation: The proposed ionization crystal cooling could be used at some later stages of the collider scheme (*e.g.*, for the final cooling), because of 'favorable' energy scaling of the relevant cooling characteristics, α, Λ, and ϵ. They can be summarized as follows:

$$\alpha \sim \gamma^{-3/2} \quad , \tag{16}$$

$$\Lambda \sim \log \gamma \quad , \tag{17}$$

and

$$\epsilon_N^{min} = \Lambda\alpha \sim \left(\gamma^{-3/2}\right) \log \gamma \quad . \tag{18}$$

Therefore, the proposed cooling mechanism scaled to higher energies looks even more attractive.

CONCLUSIONS

We have discussed the importance of a low-energy $\mu^{+}\mu^{-}$ collider that will be a Higgs factory. We do not believe that there will be any compelling need for a higher energy $\mu^{+}\mu^{-}$ collider until the results of the experiments at the LHC are obtained. A crucial requirement is to cool the $\mu^{\pm}$ to a very cold beam temperature. There are several ways one might do this, *e.g.*, starting with a friction-cooled, low-energy beam. However, we have discussed another method here that uses crystal cooling. While this is a long shot, it may be the key to reducing the beam phase-space for the precision Higgs collider application.

ACKNOWLEDGMENTS

I wish to thank members of the CMS collaboration, the U.S. $\mu^+\mu^-$ consortium, and V. Barger, J. Gunion, and T. Han for helpful comments. I also wish to thank J. Wurtle and R. Fernow for discussions, and S. A. Bogacz and D. S. Sanders for their work on ultracold $\mu^{\pm}$ beams reported here. Stimulating comments from S. Geer and P. Chen are also acknowledged.

REFERENCES

1. *Physics Potential and Development of* $\mu^+\mu^-$ *Colliders* (Proc., 2nd workshop, Sausalito, CA, 1994), ed. D. Cline, New York: AIP Conference Proceedings 352, 1995.
2. Cline, D., *Nucl. Instrum./Meth A* **350**, 24 (1994), and the following 4 papers [*Nucl. Instrum./ Meth. A* **350**, 27-56 (1994)] constitute a mini-proceedings of the Napa (Dec. 1992) meeting.
3. Rubbia, C., McIntyre, P., and Cline, D., in *Proceedings of the Int. Neutrino Conf.* (Aachen, 1976), eds. H. Faissner, H. Reithler, and P. Zerwas, Braunschweig: Vieweg & Sohn, 1977, p. 683.
4. Early references for $\mu\mu$ colliders are: (A) Perevedentsev, E. A. and Skrinsky, A. N., in *Proceedings of the 12th Int. Conf. on High Energy Accelerators* (Fermilab, 1983), eds. R. T. Cole and R. Donaldson, p. 481; (B) Neuffer, D., *Part. Accel.* **14**, 75 (1984) 75; (C) Neuffer, D., in *Advanced Accelerator Concepts*, New York: AIP Conference Proceedings 156, 1987, p. 201.
5. Neuffer, D. V., *Nucl. Instrum./Meth. A* **350**, 27 (1994).
6. For important references, see Dawson, S., Gunion, J. F., Haber, H. E., and Kane, G. L., *The Physics of the Higgs Bosons: Higgs Hunter's Guide*, Menlo Park, CA: Addison Wesley, 1989.
7. Barger, V., *et al.*, in *Physics Potential & Development of* $\mu^+\mu^-$ *Colliders* (Proc., 3rd Int. Conf., San Francisco, 1995), ed. D. Cline, *Nucl. Phys. B (PS)* **51A**, 13 (1996).
8. See papers in *Physics Potential & Development of* $\mu^+\mu^-$ *Colliders* (Proc., 3rd Int. Conf., San Francisco, 1995), ed. D. Cline, *Nucl. Phys. B (PS)* **51A** (1996).
9. "$\mu^+\mu^-$ Collider A Feasibility Study" ("Snowmass Book"), report nos. BNL-52503, Fermi Lab-conf.-96/092, LBNL-38946 (July 1996).
10. CMS Proposal for the LHC, CERN (1994), unpublished.
11. Cline, D., "Physics Potential and Development of $\mu^+\mu^-$ Colliders," UCLA preprint no. CAA-0115-12/94 (1994).
12. Cline, D., in *Beam Dynamics and Technology Issues for* $\mu^+\mu^-$ *Colliders* (Proc., 9th Advanced ICFA Beam Dynamics Wksp., Montauk, LI, NY, 1995), ed. J. C. Gallardo, New York: AIP Conference Proceedings 372, 1996, p. 279.
13. Norum, B. and Rossmanith, R., in *Physics Potential & Development of* $\mu^+\mu^-$ *Colliders* (Proc., 3rd Int. Conf., San Francisco, 1995), ed. D. Cline, *Nucl. Phys. B (PS)* **51A**, 191 (1996).
14. Skrinsky, A., in *Physics Potential & Development of* $\mu^+\mu^-$ *Colliders* (Proc., 3rd Int. Conf., San Francisco, 1995), ed. D. Cline, *Nucl. Phys. B (PS)* **51A**, 201 (1996).

15. Nagamine, K., in *Physics Potential & Development of* $\mu^+\mu^-$ *Colliders* (Proc., 3rd Int. Conf., San Francisco, 1995), ed. D. Cline, *Nucl. Phys. B (PS)* **51A**, 115 (1996).
16. Bogacz A., and Cline, D. B., in *Physics Potential & Development of* $\mu^+\mu^-$ *Colliders* (Proc., 3rd Int. Conf., San Francisco, 1995), ed. D. Cline, *Nucl. Phys. B (PS)* **51A**, 90 (1996).
17. Cline, D. B, in *Advanced Accelerator Concepts*, ed. P. Schoessow, New York: AIP Conference Proceedings 335, 1994, p. 659.
18. Fernow, R., Brookhaven National Laboratory (1995), private communication.
19. Bogacz, S. A., and Cline, D. B, *Int. J. Mod. Phys. A* **11**, 2613 (1996).
20. Bogacz, S. A., Cline, D. B., and Sanders, D. A., in *Proceedings Relativistic Channeling Wksp.*(Aarhus, Denmark, July 1995), ed. H. H. Andersen, *NIMB*, **119** (1,2), 206-209 (1996).
21. Gibson, W. M., in *Relativistic Channeling*, NATO ASI Series, vol. 165B, ed. R. A. Carrigan, Jr. and J. A. Ellison, New York: Plenum, 1986, p. 27.
22. Biryukov, V. M., *Phys. Rev. Let. E.* **51**, 3522 (1995).
23. Tsyganov, E. N., Fermilab internal report no. TM-682 (1976).
24. Bogacz, S. A., and Cline, D. B., "A Bent Crystal Undulator to Provide Gold Positron Beams," UCLA report no. CAA-0123, *NIMB* (1996), submitted.
25. Skrinsky, A. N., and Parakhomchuk, V. V., *Sov. J. Part. Nucl.* **12**, 223 (1981).